Marine Pollution Bulletin
March 2023, Volume 188 Pages 114642 (12p.)
https://doi.org/10.1016/j.marpolbul.2023.114642
https://archimer.ifremer.fr/doc/00819/93118/

Characteristics of metal pollution and multi-isotopic signatures for C, Cu, Zn, and Pb in coastal sediments from special management areas in Korea

Jeong Hyeryeong [1, 2], Lee Yeonjung [3], Moon Hyo-Bang [4], Ra Kongtae [1, 5, *]

[1] Marine Environmental Research Center, Korea Institute of Ocean Science and Technology (KIOST), Busan 49111, Republic of Korea
[2] Ifremer, RBE/CCEM, F-44000 Nantes, France
[3] Marine Ecosystem Research Center, Korea Institute of Ocean Science and Technology (KIOST), Busan 49111, Republic of Korea
[4] Department of Marine Sciences and Convergent Technology, College of Science and Convergence Technology, Hanyang University, Ansan 15588, Republic of Korea
[5] Department of Ocean Science (Oceanography), KIOST School, University of Science and Technology (UST), Daejeon 34113, Republic of Korea

* Corresponding author : Kongtae Ra, email address : ktra@kiost.ac.kr

Abstract :

The concentrations and isotopic compositions of carbon (C), copper (Cu), zinc (Zn), and lead (Pb) in coastal sediments were analyzed to identify potential pollution sources. High concentrations of total organic carbon (TOC) and metals were found close to cities and industrial areas. The isotopic compositions of C, Cu, Zn, and Pb tended to decrease as their concentrations increased. Bi-plots between δ65Cu and δ66Zn showed that the isotopic compositions in most coastal sediments, except sediments around a smelter, were similar to the isotopic compositions of road dust in urban and industrial areas of Korea. Our results suggest that heavy metal pollution in coastal sediments is greatly influenced by the pollution source, such that most metals originate from traffic and industrial activities in the urban environment. This analysis of multiple isotopes provides insights concerning the transport mechanisms and clarifies potential sources of metal contamination in coastal environments.

Graphical abstract

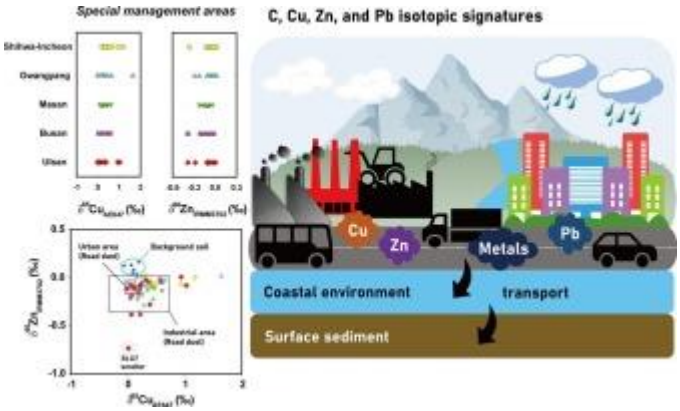

Highlights

► Metal contents and C, Cu, Zn, and Pb isotopes in coastal sediments were analyzed. ► Contaminated sediments had lighter isotopic compositions of C, Cu, Zn, and Pb. ► Metal contamination in coastal regions was highly related to traffic activities. ► Isotopic signatures can be used to manage metal contamination in coastal environment.

Keywords : Metal stable isotopes, Carbon isotope, Source identification, Marine pollution, Heavy metals

1. Introduction

Essential metals (copper (Cu), zinc (Zn), and nickel (Ni)) are important micronutrients in the marine environment; insufficient concentrations of these micronutrients may limit the growth of aquatic organisms (Posacka et al., 2017). However, concentrations above certain thresholds have toxic effects (Maldonado et al., 2006; Dong et al., 2015). Cadmium (Cd), lead (Pb), arsenic (As), and mercury (Hg) are non-essential metals that are unnecessary for living organisms; they have toxic effects with fatal consequences (Ali and Khan, 2018; Rahman and Singh, 2019). Heavy metals in the environment are of concern because of their persistence, toxicity, and bioaccumulation through food chains. Therefore, heavy metal pollution is a serious environmental problem; it has detrimental effects on the environment and ecosystems (Briffa et al., 2020; Dytlow and Gorka-Kostrubiec, 2021; Yang et al., 2018; Pandiyan et al., 2021). Because of rapid urbanization and industrialization worldwide, human activities such as industry, transportation, agriculture, and tourism have been continuously emitting metal pollution in the environment for several decades (Adnan et al., 2022; Jeong and Ra, 2022; Huang et al., 2018; Wu et al., 2020).

Heavy metals present in the terrestrial environment are discharged into the coastal environment through various transport pathways, such as rivers, streams, atmospheric deposition, and sewage or wastewater treatment plant outlets (Guan et al., 2018; Ji et al., 2019; Kinuthia et al., 2020). Among these pathways, point sources such as the discharges from sewage and wastewater treatment plants can be managed by increasing the treatment capacities of such plants. However, it is difficult to manage and control non-point pollution sources because they accumulate on impervious surfaces in the urban environment and are discharged without any treatment. An important non-point source of land-based metal pollution is road dust, which accumulates in impervious areas such as paved roads, buildings, and parking lots in urban and industrial regions (Jeong et al., 2020a; Jeong and Ra, 2022; Suvetha et al., 2022). Stormwater runoff resuspends small particles of road dust with a high metal concentration; large amounts of heavy metals are discharged directly into the coastal environment through sewers and rivers together with runoff (Huber et al., 2016; Hwang et al., 2016; Jeong et al., 2021a; 2021b).

In Korea, many cities and national industrial complexes are concentrated in coastal areas. Although this concentration provides many economic advantages, it also causes serious environmental problems such as water quality deterioration and heavy metal pollution. To address these environmental problems, the Korean government has designated five coastal areas as special management areas (SMAs) where specific efforts are made to support environmental conservation and management. The recently introduced total pollution load management system has slightly improved the management of some environmental concerns, such as eutrophication and oxygen depletion, in bottom water (Jun et al., 2018; Park et al., 2018). However, coastal areas with active urban and industrial activities continue to show extensive heavy metal contamination in Korea (Ra et al., 2011; 2014). Road dust in urban and industrial

areas near SMAs is extremely polluted with heavy metals (Jeong et al., 2020c). Heavy metal pollution in coastal SMAs is severely affected by traffic and industrial activities that occur in nearby terrestrial areas, and substantial amounts of heavy metals are discharged through non-point pollution sources (Jeong et al., 2020b; 2021b; Jeong and Ra, 2021a). It has been difficult to manage the heavy metal pollution issues in SMAs; there is a need for comprehensive monitoring of metal concentrations and the implementation of a total pollution load management system centered on organic matter.

The analysis of metal and organic matter concentrations alone has many limitations in identifying specific sources of environmental pollution in coastal environments. Despite the complexity of environmental pollution, organic matter and metal pollution have been conducted separately in many studies. The most effective environmental conservation and management policies involve controlling potential sources of both metals and organic pollutants before they enter coastal areas. Due to the unique isotopic signatures of the substances, stable isotope studied are becoming increasing important as a powerful tool to provides new insight in many environmental fields (Araújo et al., 2022; Wang et al., 2021a; Wiederhold, 2015). Stable carbon (C) isotope researches enable to identify different emission sources by reflecting isotope fractionations related to the generation processes of the source material (Zimnoch et al., 2020; Kim et al., 2021). Metal stable isotopes such as Cu, Zn, and Pb are used to understand geochemical processes, behavior in biological system, and to distinguish the natural and anthropogenic sources of metal pollution in the environment (Bird, 2011; Desaulty and Petelet-Giraud, 2020; Wang et al., 2017; Yin et al., 2016). The application of stable isotopes of multi-elements rather than single element will provide more scientific information for solving environmental issues. Recently, studies on the stable isotope for multi-elements have been started to identify contamination sources as powerful scientific evidence in environmental forensic fields (Barre et al., 2018; Vanderstraeten et al., 2020; Pontér et al., 2021).

The purpose of this study is (1) to evaluate the heavy metal pollution status and ecological risks in surface sediments from five different SMAs in Korea; (2) to identify metal pollution sources in coastal areas using the multi-isotopic signatures of C, Cu, Zn, and Pb. This study can be helpful in managing and reducing environmental pollutants through understanding the potential sources of metal pollution in coastal environments. Additionally, concentration and isotope data of this study will serve as important information for decision makers in environmental policy.

2. Materials and methods

2.1. Study area

The Shihwa-Incheon SMA is located in the western part of Korea. Many industrial complexes and large cities (e.g., Incheon, Ansan, and Siheung) are located in the basin. Gwangyang and Masan SMAs are located in the southern part of Korea. Busan SMA is located in the southeastern corner of Korea and is

the largest port city; its population is approximately 3.5 million. Ulsan SMA is located in the southeastern part of Korea; it is the site of several heavy industry-related national industrial complexes, such as Ulsan-Mipo and Onsan. The Shihwa-Incheon SMA has the largest managed sea area of 605 km^2; this is followed by Busan (236 km^2), Masan (143 km^2), Gwangyang (131 km^2), and Ulsan (57 km^2). The managed land basin area is 1.5-fold larger than the managed sea area; several large national industrial complexes and cities are located in the vicinity of the SMAs.

2.2. Sampling and metal analysis

For each SMA region, 10 sampling sites were selected, and a total of 50 surface sediment sampling from 5 SMAs was conducted using a grab sampler in 2020 (Fig. 1). The collected samples were immediately frozen with dry ice and transported to the laboratory. Freeze-dried samples were pulverized and homogenized using a planetary mono mill grinder (Pulverisette 6, Fritsch Co., Markt Einersheim, Germany), then stored for subsequent chemical analysis. After homogenized samples had been decomposed by the total acid digestion method using a high-purity acid mixture (HF, HNO_3, $HClO_4$; Ra et al., 2011), the concentrations of aluminum (Al) and trace metals (vanadium (V), Cr, Co, Ni, Cu, Zn, As, Cd, antimony (Sb), and Pb) were determined by inductively coupled plasma mass spectrometry (iCAP-Q, Thermo Fisher Scientific, Germany) at the Korea Institute of Ocean Science and Technology (KIOST). The Hg concentration was determined using a mercury analyzer (DMA-80, Milestone Inc., Milan, Italy). To validate the accuracy of the metal analysis in this study, two types of certified reference materials (MESS-4 and BCR667) were used. The recoveries of the reference materials ranged from 95.9% (As) to 101.6% (Sb) for MESS-4 and from 94.5% (Zn) to 99.2% (V) for BCR667. Results consistent with certified values were obtained. All 50 sediment samples were subjected to particle size analysis with a laser particle size analyzer (Mastersizer 2000, Malvern Ltd., Malvern, UK) after the removal of inorganic carbon and organic matter with 1 N HCl and H_2O_2 (Kanto Chemical Co., Tokyo, Japan), respectively.

2.3. Total organic carbon (TOC) and carbon isotope analysis

After HCl treatment to remove inorganic carbon, the organic carbon concentration was determined by an elemental analyzer (Euro EA3028, EuroVector, Milan, Italy). The isotopic compositions of carbon ($\delta^{13}C$) were determined by an isotope ratio mass spectrometer (Isoprime, GV Instruments, Altrincham, UK) at the KIOST. The measured $\delta^{13}C$ values were determined from the isotopic composition of Vienna Pee Dee Belemnite (VPDB) as a per mil (‰) deviation.

$$\delta^{13}\mathrm{C}\ (‰) = \left(\frac{\left(^{13}\mathrm{C}/^{12}\mathrm{C}\right)_{\mathrm{sediment}}}{\left(^{13}\mathrm{C}/^{12}\mathrm{C}\right)_{\mathrm{VPDB}}} - 1 \right) \times 1000$$

2.4. Stable isotope analyses of Cu, Zn, and Pb

For stable isotope analyses, Cu and Zn were purified from sediment samples by column separation using an anion exchange resin (AG-MP1, 100–200 mesh, Bio-Rad, Hercules, CA, USA). Pb was separated from the sediment matrix using a Pb-specific resin (100–150 μm particle size, Eichrom, Lisle, IL, USA). The analytical procedure and instrumental settings for the isotope analyses of Cu, Zn, and Pb were described in detail by Jeong et al. (2021c). After column separation and adjustment of sample concentrations to within 5% (100 ppb for Cu and 200 ppb for Zn), the isotopic compositions for Cu and Zn were determined by multi-collector inductively coupled plasma mass spectrometry (MC-ICP-MS; Neptune Plus, Thermo Fisher Scientific, Germany) at the KIOST.

The Cu and Zn isotopic compositions (δ^{65}Cu and δ^{66}Zn) were expressed as a per mil (‰) deviation relative to the isotopic standards for Cu (ERM-AE647, Institute for Reference Materials and Measurements (IRMM), Belgium) and Zn (IRMM-3702, IRMM, Belgium):

$$\delta^{65}\mathrm{Cu}\ (‰) = \left(\frac{\left(^{65}\mathrm{Cu}/^{63}\mathrm{Cu}\right)_{\mathrm{sediment}}}{\left(^{65}\mathrm{Cu}/^{63}\mathrm{Cu}\right)_{\mathrm{AE647}}} - 1\right) \times 1000$$

$$\delta^{66}\mathrm{Zn}\ (‰) = \left(\frac{\left(^{66}\mathrm{Zn}/^{64}\mathrm{Zn}\right)_{\mathrm{sediment}}}{\left(^{66}\mathrm{Zn}/^{64}\mathrm{Zn}\right)_{\mathrm{IRMM3702}}} - 1\right) \times 1000$$

In order to compare with previously reported values, the δ^{65}Cu and δ^{66}Zn values of NIST SRM976 and JMC-Lyon were converted to ERM-AE647 and IRMM-3702, respectively (Moeller et al., 2012; Araújo et al., 2017a):

$$\delta^{65}Cu_{ERM-AE647} = \delta^{65}Cu_{NIST976} - 0.21‰$$

$$\delta^{66}Zn_{IRMM3702} = \delta^{66}Zn_{JMC} - 0.27‰$$

The Pb isotopes (^{204}Pb, ^{206}Pb, ^{207}Pb, and ^{208}Pb) were also determined by MC-ICP-MS at the KIOST. During isotope measurements, instrumental bias correction was performed using a Zn (IRMM-3702) addition for Cu, a Cu (ERM-AE647) addition for Zn, and a Tl addition (NIST SRM 997, USA) for Pb. The standard-sample bracketing method was used for the calibration and correction of instrumental bias during isotope analysis. Isotope data were measured three times for each sample and the mean values were recorded. All chemical procedures and analyses conducted in this study were performed in a clean room (class 1,000) at the KIOST.

The accuracy of the isotope analysis was checked using the in-house standard solutions and certified reference materials (CRMs). For in-house solutions, the isotopic compositions were –0.21±0.03‰

(AE633; 2sd, n=9) and +0.11±0.03‰ (Kanto solution; 2sd, n=9) for $\delta^{65}Cu_{AE647}$ and –11.58±0.03‰ (IRMM-651; 2sd, n=9) and –0.07±0.02‰ (Kanto solution; 2sd, n=9) $\delta^{66}Zn_{IRMM3702}$, respectively. These in-house solutions were analyzed before, middle, and at the end of sample analysis, and the isotopic compositions were consistent with previously reported values (Jeong et al., 2021c). Two types of CRMs (MESS-4 and BCR667) were treated by the same procedure as the sediment samples to confirm isotope fractionation that may occur during column separation, and isotope analysis for Cu, Zn, and Pb was also conducted. The measured isotopic compositions were –0.03±0.03‰ (MESS-4; 2sd, n=3) and +0.06±0.04‰ (BCR667; 2sd, n=3) for $\delta^{65}Cu_{AE647}$, –0.01±0.01‰ (MESS-4; 2sd, n=3) and –0.05±0.01‰ (BCR667; 2sd, n=3) for $\delta^{66}Zn_{IRMM3702}$, and 1.2266±0.0003 (MESS-4; 2sd, n=3) and 1.1812±0.0003 (BCR667; 2sd, n=3) for Pb ($^{206}Pb/^{207}Pb$), indicating within good agreement with previously reported values (Jeong et al., 2021c).

2.5 Pollution assessments

The enrichment factor (EF) is widely used to assess the degree of pollution for individual metals. Because the EF is normalized to the concentration of a conservative element, it is possible to reduce the effects of differences in mineral composition and particle sizes of the sediments. In this study, the EF was normalized using the Al concentration by using the following equation (Zolle et al., 1974):

$$EF = {(metal/Al)_{sediment}}/{(metal/Al)_{background}}$$

The background values for each metal were adopted from the work by Rudnick and Gao (2003). The EF value is classified into six classes from depletion to minimum enrichment (EF < 2) to extremely high enrichment (EF > 40) (Sutherland, 2000).

The pollution load index (PLI) was calculated to evaluate the overall contamination levels of the 11 heavy metals measured in this study by using the following equation (Tomlinson et al., 1980):

$$PLI = (PI_1 \times PI_2 \times PI_3 \ldots \times PI_{11})^{1/11}$$

where PI is the ratio of heavy metal concentration in the sediment to the background value. A PLI value > 1 indicates the presence of anthropogenic contamination.

3. Results and discussion

3.1. Particle size, TOC, and heavy metal concentrations in sediments

The mean, minimum, maximum, and coefficient of variation (CV) of particle size, TOC, and heavy metal concentrations in the sediments are shown in Table 1. The mean particle size and CV in Ulsan were 14 μm and 23%, respectively; the fine-grained sediments were uniformly distributed. In

Gwangyang and Shihwa-Incheon, the mean particle sizes were 63 and 51 μm, respectively; the CV also exceeded 100%. Compared to other regions, more coarse sediments were deposited in Gwangyang and Shihwa-Incheon; the particle sizes greatly differed according to sampling site (Fig. 2). The mean TOC concentration was 1.19% (range, 0.08% to 2.86%). The mean TOC concentration in Masan was 1.92%, which was approximately 4.4-fold greater than the concentration in Shihwa-Incheon.

The mean Hg, Cd, Sb, As, Co, Ni, Pb, Cu, Cr, V, and Zn concentrations in the sediments were 0.14, 0.35, 1.1, 9.2, 11.5, 24.6, 40.2, 52.8, 58.0, 75.1, and 150 mg/kg, respectively. The mean CV values of heavy metals in the sediments decreased in the following order: Hg (239%) > Cu (109%) > Cd (93%) > Sb (80%) > Pb (79%) > Zn (61%) > Co (50%) > As (40%) > Ni (28%) > Cr (25%) > V (24%). Both Hg and Cu had CV values > 100%. Cd, Sb, Pb, and Zn also had high CV values that ranged from 61% to 93%. These results suggested that metal deposition in sediment varied among sampling sites and was affected by anthropogenic activities. The CV values of Co, As, Ni, Cr, and V—for which there were small differences in mean concentration among the five SMA regions—were < 50%, indicating that the influence of a natural (rather than anthropogenic) origin was dominant.

The mean Co, Ni, As, Sb, Pb, and Hg concentrations were higher in sediments from Ulsan than in sediments from other regions. The highest Zn, Cd, Pb, and Hg concentrations were observed in sediments from site U7 around the Onsan industrial complex, which contains the largest smelting facilities in Korea. In this area, raw materials from the smelting industry have spilled on to the road surface during transportation; this has resulted in high heavy metal concentrations in road dust close to the smelter (Jeong et al., 2021b). The surrounding environment, including stream and marine sediments, is also heavily contaminated with heavy metals (Jeong et al., 2021a). Furthermore, many ports in the area are used to import raw materials for the surrounding heavy industry. Therefore, metal contamination in Ulsan is mainly caused by industrial activities and traffic activities, such as the transportation of raw materials using trucks or ships.

The mean concentrations of V, Cr, Cu, and Zn were higher in sediments from Busan than in sediments from other regions. The highest Cu concentration was identified at site B7, where shipbuilding and ship repair facilities are concentrated. Busan is the second largest city in Korea and has many harbors. Both Cu and Zn are widely used in antifouling paints (APs) that are applied to ships. In the harbor area, Cu and Zn are released from APs into the seawater, then deposited (in small amounts) in sediments during ship repair activities. These activities consequently contaminate the seawater and sediments in the harbor environment with Cu and Zn (Schiff et al., 2004; Pourabadehei and Mulligan, 2016; Lagerström et al., 2020). The surface sediments in Busan have high concentrations of Cr and Sb. The harbor area directly receives surface runoff from the urban area. Therefore, metal contamination in Busan is affected by both traffic and shipping activities. Similar to TOC, the highest mean value of Cd (0.65 mg/kg) was

found in Masan. Cd concentrations are reportedly higher in road dust from industrial areas located inside Masan Bay than in other industrial areas in Korea (Albuja et al., 2022).

The Shihwa-Incheon and Gwangyang areas had the lowest concentrations of most heavy metals, along with large particle sizes in surface sediment. Although the national industrial complex and many cities are located in these areas, contaminated fine sediments derived from urban environments might have been discharged to the outer sea. In most of the studied areas, heavy metal concentrations were high at sampling sites close to the cities and industrial facilities; they tended to decrease toward the outer sea. These results indicate that heavy metal contamination in the SMAs of Korea is strongly affected by human activities (e.g., traffic and industrial processes) from the land area, along with shipping activities in the coastal area.

3.2. Heavy metal pollution assessment

The mean EFs for heavy metals in sediments from the five SMAs are shown in Table 2. The mean EFs of heavy metals from the Shihwa-Incheon and Gwangyang areas were < 2, which indicated depletion to minimum enrichment. Most heavy metals in these areas originated from natural sources. However, in the Shihwa-Incheon area, Pb levels were in the moderate enrichment class at sites S1 and S2 close to Incheon metropolitan city, while the EFs of Cd at sites S8 and S9 near the industrial complex ranged from 2 to 5, indicating moderate enrichment. Gwangyang also exhibited moderate enrichment of Pb at sites G1, G3, and G4, which were the locations of industrial facilities. The mean EF of Cd in the Masan area showed moderate enrichment, but significant enrichment was observed at sampling sites M1–M5, where EFs were > 5. In the Busan area, Cu had the highest mean EF value of 3.5, which corresponded to moderate enrichment. The mean EFs of Zn, Cd, Sb, and Pb ranged from 2 to 5, indicating that these metals were also moderately enriched. At sampling sites where ship repair work was conducted, the EF of Cu was > 5, which represented significant enrichment. The EF of Sb was 8.1 at site B4, where a large fish market and downtown area were located, indicating contamination by traffic activity in the form of brake pad debris. In the Ulsan area, the mean EF of Hg was 10.7, which was the highest value among the 11 heavy metals. The EF of Hg was > 40 at two sampling sites (U5 and U7), indicating extremely high enrichment. The highest EF values of Cu (11.9), Zn (9.9), Cd (26.6), Sb (12.2), and Pb (20.1) were observed at site U7, which was near a stream connected to the smelter. These results indicated that substantial amounts of heavy metals from the smelting industry had accumulated in marine sediment through rainfall runoff. A comparison of the PLI among regions is shown in Fig. 2. Ulsan had the highest PLI value (2.0); this was followed by Busan > Masan > Shihwa-Incheon > Gwangyang. The PLI value was > 1 for most sampling sites from the Ulsan, Busan, and Masan areas, implying that the sediments had been contaminated by heavy metals. The mean PLI values of the Shihwa-Incheon and Gwangyang areas were < 1, indicating low contamination levels. Our results suggested that sediments in the SMAs

of Korea were substantially affected by heavy metal contamination from neighboring urban and industrial areas.

3.3. Isotopic compositions of C, Cu, Zn, and Pb

The isotopic compositions of C, Cu, Zn, and Pb and a regional comparison are shown in Table 3 and Fig. 2. The sediments from Ulsan had a depleted mean $\delta^{13}C$ value of –22.69‰ (range, –25.72‰ to –20.98‰). The $\delta^{13}C$ values of the sediments from Masan varied between –27.07‰ and –20.43‰; depleted values (–27.07‰ to –23.61‰) were found inside Masan Bay near the urban area. The difference in $\delta^{13}C$ values between the Shihwa-Incheon and Gwangyang areas was small, with mean values of –21.80‰ and –21.57‰, respectively. Because the $\delta^{13}C$ values in coastal sediments reflect the isotopic compositions of carbon sources, they can be used to distinguish between marine and terrestrial sources in sediments (Alonso-Hernandez et al., 2020; Mao et al., 2021). Generally, $\delta^{13}C$ values tend to be lower in terrestrial sources than in marine sources (Kwon et al., 2021; Marwick et al., 2015). Sampling sites affected by terrestrial inputs near cities and industrial facilities generally had depleted $\delta^{13}C$ values. The $\delta^{13}C$ values in sediments tended to increase from the inside of the bay to the outer sea. The $\delta^{13}C$ values in sediments of Shihwa, where seawater exchange was restricted by a sea dike, were more depleted than $\delta^{13}C$ values in sediments of Incheon, which was connected to the outer sea. Lee et al. (2014) found that samples collected in the rainy season had more depleted $\delta^{13}C$ values than did samples collected in the dry season; the contributions of human activities in urban and industrial areas tended to increase during the rainy season. They concluded that the organic matter inputs from anthropogenic activity in terrestrial areas were strongly influenced by heavy rainfall. Our results also showed a high TOC concentration and depleted $\delta^{13}C$ values in sediments close to the highly urbanized and industrialized areas, suggesting the influence of anthropogenic inputs from the terrestrial area.

The $\delta^{65}Cu$ values were positive except at one sampling site (U3); the overall variation in $\delta^{65}Cu$ values was ~1.65‰ (Table 3). The mean $\delta^{65}Cu$ values in sediments were +0.52‰ from Shihwa-Incheon, +0.40‰ from Gwangyang, +0.30‰ from Masan, +0.25‰ from Busan, and +0.32‰ from Ulsan. The $\delta^{65}Cu$ values in sediments from Gwangyang ranged from +0.00‰ to +1.64‰. The $\delta^{65}Cu$ values were highest in sediments from Shihwa-Incheon. The mean $\delta^{65}Cu$ value in this study was higher than the mean values in road dust from industrial areas (+0.03‰; Jeong et al., 2021a), urban areas (+0.05‰; Jeong and Ra, 2021b), background soil (+0.09‰, Jeong and Ra, 2021b), and stream sediments (+0.17‰, Jeong et al., 2020d) in Korea. The sediments from Busan had the lowest mean $\delta^{65}Cu$ value (+0.25‰), which was similar to the value in brake pads produced in Korea (+0.15‰; Jeong et al., 2022a). Brake pads contain up to 12% Cu (Jeong et al., 2022a); thus, they constitute a major source of contamination in urban road dust. The Cu isotopic composition of tires in Korea, which is one of the most important non-exhaust emission sources, was reported –0.51‰ (Jeong, 2022). The $\delta^{65}Cu$ values were generally

low in sampling sites close to the cities and industrial complexes. In industrial areas, traffic activity is lower than in urban areas; however, there are many heavy-duty vehicles (e.g., trucks and trailers). Compared with light-duty vehicles, heavy-duty vehicles emit more particles from brake pad wear on the road surface (Bukowiecki et al., 2009). Additionally, the road dust with the highest Cu concentrations from industrial areas of Korea (where Cu smelters, refineries, and Cu alloy manufacturers are concentrated) reported a δ^{65}Cu value of –0.33‰ (Jeong and Ra, 2021a). Therefore, the Cu contamination in sediments was influenced by industrial and traffic activity.

The mean δ^{66}Zn value in the sediments was –0.12‰ (range, –0.73‰ to +0.02‰). There was generally minimal variation in δ^{66}Zn values, in contrast to the δ^{65}Cu values (Table 3). The Zn isotopic composition in Masan was –0.12‰, with lower relative variability than the other areas (Fig. 2). The highest δ^{66}Zn values were observed at sampling sites G4 (+0.02‰) and G9 (+0.01‰) in Gwangyang and at sampling site S6 (+0.02‰) in Shihwa-Incheon. The mean δ^{66}Zn value in the sediment from Ulsan was –0.19‰, which was lower than in other areas; substantial variation in Zn isotopic composition was also observed because δ^{66}Zn values were lowest in the vicinity of the smelter (site U7), where the Zn concentration was extremely high. Araújo et al. (2017b) reported that Zn isotopic compositions (converted to IRMM-3702) in the willemite ore (Zn_2SiO_4) range from –0.37‰ to –0.13‰; they have lighter values, compared to sediment cores (+0.03 to +0.88‰). Their study also showed that anthropogenic Zn sources in urban and industrial areas had a light Zn isotopic composition (Araújo et al., 2021). The Zn content in Korean tires is reportedly 1.4% and the Zn isotopic composition has a mean of –0.06‰ (range, –0.09‰ to –0.03‰) (Jeong, 2022). The δ^{66}Zn values in brake pads have been reported to range from –0.09‰ to +0.03‰ (Jeong et al., 2022a). The Zn concentration was much lower in coastal sediments than in non-exhaust emission sources (e.g., road dust in urban and industrial areas), although the Zn isotopic compositions had similar values. However, the Zn isotopic composition in coastal sediments was lower than the mean δ^{66}Zn value in the background soil of Korea. Similar to Cu, Zn is affected by traffic-derived pollution sources. However, our results indicated that, compared with Cu isotopes, the Zn isotopic composition in sediments is better able to preserve the industrial pollution record.

Non-exhaust traffic emissions (NEEs) reported by Schleicher et al. (2020) included road tunnel PM_{10}, road dust, road furniture, brakes, and tires and the corresponding NEEs used in this study were brakes, tires, road dust from industrial and urban areas. The Zn isotopic composition in NEEs of this study was within the range reported by Schleicher et al. (2020). However, the Cu isotope composition had a wider range than the values reported by Schleicher et al. (2020) due to the relatively low Cu isotopic compositions in tires and the high Cu isotopic values of road dust in the industrial area. Souto-Oliveira et al. (2019) reported the Zn isotopic composition (converted to IRMM-3702; $\delta^{66}Zn_{IRMM3702}$) in tires was –0.11±0.14 ‰ (2sd, n=9), indicating a relatively heavier isotopic composition than that of Korean products. Isotopic compositions can vary depending on different manufacturers and origins of raw

materials (Jeong, 2022; Jeong et al., 2022a). Industrial emissions can reveal lighter Zn isotopic compositions (converted to IRMM3702; $\delta^{66}Zn_{IRMM3702} < -0.87‰$) (Souto-Oliveira et al., 2018; 2019), however, urban aerosol had relatively heavier Cu and Zn isotopic compositions (Souto-Oliveira et al., 2018). Ulsan region of this study, most strongly affected by industrial activities, showed the lightest Zn isotopic compositions ($\delta^{66}Zn_{IRMM3702}$: –0.73‰). Relatively heavier isotopic compositions of Cu and Zn seem to be more related to traffic activities in the urban city.

The Pb isotopic composition, expressed as the $^{206}Pb/^{207}Pb$ isotopic ratio in the sediments, varied between 1.1006 and 1.1924 (Table 3). For the $^{206}Pb/^{207}Pb$ isotopic ratio in sediments, the Gwangyang (1.1820) and Ulsan areas (1.1641) had more radiogenic and less radiogenic mean values, respectively. Less radiogenic $^{206}Pb/^{207}Pb$ value of 1.1006 was recorded at site U7, which had the highest Pb concentration (232 mg/kg); there were substantial isotopic differences among the sampling sites. Anthropogenic Pb pollution sources reportedly have lower $^{206}Pb/^{207}Pb$ ratios; the values in brake pads and tires in Korea are 1.2398 and 1.1568, respectively (Jeong et al., 2022a; Jeong, 2022). Similar to the Zn isotopes, the variation of Pb isotopic composition was the least in the Masan area (Fig. 2). The $^{206}Pb/^{207}Pb$ value in coastal sediments was more radiogenic than in road dust of urban (1.1514) and industrial (1.1538) areas, but it was slightly less radiogenic than in background soil (1.1827) (Jeong and Ra, 2021a; 2021b).

3.4. Identification of metal sources in coastal sediments

Heavy metals in coastal environments are supplied in dissolved and particulate phases from the terrestrial area. When dissolved metals enter into the coastal environments through river discharge, outfalls from wastewater treatment plants (WWTPs), sewers, and wet deposition, metals in a dissolved phase are easily attached to suspended particulate matter (SPM) and then deposited into bottom sediments due to strong affinity for particles (La Colla et al., 2015; Feng et al., 2017). Additionally, surface soils, river sediments, and road-deposited sediments contaminated with heavy metals are directly transported into the coastal environment via stormwater runoff and dry deposition (Wicke et al., 2012; Jeong et al., 2020b).

Pearson correlation analysis was performed to determine the source of metal pollution through the relationship between concentration and isotopic composition for C, Cu, Zn, and Pb. Heavy metals in sediments exist in various phases, including labile (exchangeable), organic-bound, carbonate-bound, reducible (Fe-Mn oxides), and residual. In general, heavy metals in sediments have close relationships with physical and chemical parameters such as grain size and TOC; fine sediments have high organic and metal contents (Ra et al., 2014; Liu et al., 2016; Tang et al., 2018). The particle size in the sediment was negatively correlated with the TOC, V, Cr, Ni, Zn, and Sb concentrations ($p < 0.01$; Table 4). The

TOC concentration was positively correlated with V, Cr, Ni, Cu, Zn, As, Cd, and Sb concentrations ($p < 0.01$). Several studies have reported that the concentration of metals in the particulate phase of in coastal seawater and runoff was much higher than those in the dissolved phase (Jeong et al., 2020b). During precipitation, the metal concentration of particulate metals in estuarine water and surface sediments was significantly increased compared to that of dissolved metals (Jeong et al., 2022b). We propose that the discharge of particles deposited in the impervious layer from the terrestrial region rather than the scavenging from the water column is the dominant source of metal contamination in coastal sediments.

Especially, Sb, which is known to be polluted by traffic activity in urban environments, showed a positive correlation with TOC and most metals, implying that organic matter and heavy metals in coastal sediments is affected by adjacent terrestrial regions. The relationship between concentration and isotopic composition of C, Cu, Zn, and Pb is shown in Fig. 3. The $\delta^{13}C$ values tended to decrease as the TOC concentration increase and a negative correlation was observed ($p < 0.01$, $r = –0.42$). The Cu, Zn, and Pb isotopic compositions showed lower values at high concentrations. The isotopic composition correlations for Cu ($p < 0.01$, $r = –0.48$), Zn ($p < 0.01$, $r = –0.71$) and Pb ($p < 0.01$, –0.78) concentrations were all negative and the $\delta^{65}Cu$, $\delta^{66}Zn$ and $^{206}Pb/^{207}Pb$ became lighter as the concentration increased (Fig. 3 and Table 4). The sampling site close to the terrestrial regions had higher metal concentrations and lower isotopic compositions. These results suggest that metal contamination in coastal sediments is influenced by contamination sources with lighter isotopic values from adjacent terrestrial regions. It has been reported that the mean values of $\delta^{65}Cu$, $\delta^{66}Zn$, and $^{206}Pb/^{207}Pb$ in road dust (<63 μm) from the Shihwa industrial complex around Shihwa-Incheon SMA were +0.03‰, –0.13‰ and 1.1568, respectively (Jeong and Ra, 2021a). These values are lighter than those in coastal sediments from Shihwa-Incheon SMA.

Hwang et al. (2019) reported the status of metal contamination in the coastal sediments of Korea. The mean concentrations of As, Cd, Cu, Pb, and Zn in coastal sediments were 7.4, 0.09, 13.8, 24.1, and 73 mg/kg, respectively, showing lower metal concentrations than in SMA regions. The surrounding land area is larger than the SMAs, there is a large input of terrestrial pollution. The results of the correlation between TOC, metals, and isotopic compositions indicate that organic matter and metal contamination is more affected by anthropogenic activity in surrounding urban regions than specific contamination source from industrial regions.

Analyses of metal isotopes enable the separation of their different origins, including both natural and anthropogenic sources. Several studies using multiple isotopes of Cu, Zn, and Pb have been conducted to identify sources of metal pollution and understand the transport processes in atmospheric particles (Dong et al., 2017; Schleicher et al., 2020; Souto-Oliveira et al., 2019), marine sediments (Araújo et al.,

2019), and road dust (Jeong and Ra, 2021a; 2021b). Most of the coastal sediment results in this study were located in the range of road dust results from urban and industrial areas (Fig. 4a). Road dust is an important carrier of heavy metals; it is a source of suspended particles in the surrounding environment. In dry weather, pollutants accumulate in the permeable layer on land; the organic content and metal pollution levels are generally higher in fine road dust particles (Gelhardt et al., 2021; Wang et al., 2021b). During rainfall events of all magnitudes, fine road dust is easily resuspended and transported by rainfall runoff; subsequently, it disperses to coastal areas through the urban drainage system and accumulates in sediments (Jeong et al., 2020b; Wang et al., 2019; Zhao et al., 2022). Our results indicated that Cu and Zn pollution is largely caused by traffic activity for both public transportation and industrial activity. Figure 4b is a bi-plot between the δ^{66}Zn values and $^{206}Pb/^{207}Pb$ isotopic ratios. The Zn isotopic compositions were similar in road dust from urban and industrial areas, but Pb had an isotopic composition that was closer to the composition of the background soil. Considering the Pb concentrations of the sediments, Pb pollution may also be derived from other sources. In particular, the Cu concentrations in Busan, which has many operational harbors, were higher than in other regions. Considering the extremely high metal concentrations in APs and the intensive ship repair activities in the harbors, Cu pollution in Busan must have been influenced by both road dust and APs. Thus far, the isotopic composition in APs has not been reported. The isotopic compositions of the metals reflected the intensity of industrial activities such as smelters.

To fully understand and trace the origins of metal pollution in the coastal area, isotopic data should be established for as many potential sources as possible. The combined data for these metals provide useful insights that are needed to identify sources of metal pollution in coastal sediments. Additionally, the high Sb concentrations in coastal sediments close to urban areas suggested that the road dust is transported into coastal areas along with rainfall runoff. The development and application of an isotope analysis methodology for key metal pollutants (Sb, Cd, and Hg) together with Cu, Zn, and Pb will be important for effectively controlling the sources of metal pollution.

Conclusion

In the coastal environments investigated in this study, there were various sources of heavy metal pollution; metals originated from traffic, industrial, and shipping activities. The presence of increased infrastructure (e.g., paved roads and impervious areas) in relation to the expansion of urban and industrial areas is gradually increasing the terrestrial area in which human activities occur. To effectively manage the heavy metal pollution that affects the environment and local ecosystems, it is important to understand the transportation pathways and reduce heavy metals present in the urban environment before they enter the coastal environment.

This study attempted to identify sources of heavy metal pollution using the stable isotopic composition of multiple elements (e.g., C, Cu, Zn, and Pb) in coastal sediments. High metal concentrations were observed in sampling sites close to urban and industrial areas. The isotopic composition of Cu, Zn, and Pb decreased as the concentration in the sediments increased. The bi-plot results for the $\delta^{65}Cu$ and $\delta^{66}Zn$ values showed that the isotopic composition of coastal sediments was similar to the compositions of road dust in urban and industrial areas. This suggests that the heavy metals present on land are continuously supplied to the coastal environment through rainfall runoff.

Our data showed that the isotopic compositions of multiple elements (C, Cu, Zn, and Pb) in the sediments provided important information concerning the sources of heavy metal pollution in coastal areas. It was found that traffic activity in surrounding cities has been identified as a major source of metal contamination in coastal regions where metal contamination is not significant. However, lighter isotopic compositions were observed around smelters and harbors with severe metal contamination, reflecting the influence of industrial activities as well. The accumulation of isotope data for identification of additional potential sources and development of new methodologies for detection of emerging metals will help to address environmental problems related to heavy metals by estimating the relative contribution of each pollution source to the overall concentration in the environment.

CRediT authorship contribution statement

Hyeryeong Jeong: Conceptualization, Visualization, Writing-original draft, Writing-review and editing. **Yeonjung Lee:** Methodology, Writing-editing. **Hyo-Bang Moon:** Investigation, Methodology. **Kongtae Ra:** Investigation, Methodology, Writing-original draft, Writing-review and editing, Funding acquisition, Supervision

Declaration of competing interests

The authors declare that they have no known competing financial interests or personal relationships that could have influenced the work reported in this paper.

Acknowledgments

This research was supported by the “Development of source identification and apportionment methods for toxic substances in marine environments” program of the Korea Institute of Marine Science & Technology Promotion (KIMST) funded by the Ministry of Oceans and Fisheries (KIMST-20220534); it was also supported by a grant (PEA0012) from the Korea Institute of Ocean Science and Technology (KIOST).

References

Adnan, M., Xiao, B., Xiao, P., Zhao, P., Bibi, S., 2022. Heavy metal, waste, COVID-19, and rapid industrialization in this modern era—Fit for sustainable future. Sustainability 14, 4746. https://doi.org/10.3390/su14084746

Albuja, M., Jeong, H., Ra, K., 2022. Assessment of pollution, ecological and health risks of potentially toxic elements (PTEs) in road dust from Changwon industrial complex. J. Korean Soc. Mar. Environ. Energy 25(2), 1–12 (in Korean with English abstract). https://doi.org/10.7846/JKOSMEE.2022.25.2.1

Ali, H., Khan, E., 2018. Bioaccumulation of non-essential hazardous heavy metals and metalloids in freshwater fish. Risk to human health. Environ. Chem. Lett. 16, 903–917. https://doi.org/10.1007/s10311-018-0734-7

Alonso-Hernandez, C.M., Fanelli, E., Diaz-Asencio, M., Santamaria, J.M., Morera-Gemoz, Y., 2020. Carbon and nitrogen isotopes to distinguish sources of sedimentary organic matter in a Caribbean estuary. Isotopes Environ. Health Stud. 56(5-6), 654–672. https://doi.org/10.1080/10256016.2020.1819263

Araújo, D.F., Boaventura, G.R., Viers, J., Mulholland, D.S., Weiss, D., Araujo, D., Lima, B., Ruiz, I., Machado, W., Babinski, M., Dantas, E., 2017a. Ion exchange chromatography and mass bias correction for accurate and precise Zn isotope ratio measurements in environmental reference materials by MC-ICP-MS. J. Braz. Chem. Soc., 28, 225–235. https://doi.org/10.5935/0103-5053.20160167

Araújo, D.F., Boaventura, G.R., Machado, W., Viers, J., Weiss, D., Patchineelam, S.R., Ruiz, I., Rodrigues A.P.C., Babinski, M., Dantas, E., 2017b. Tracing of anthropogenic zinc sources in coastal environments using stable isotope composition. Chem. Geol. 449, 226–235. https://doi.org/10.1016/j.chemgeo.2016.12.004

Araújo, D. F., Ponzevera, E., Briant, N., Knoery, J., Bruzac, S., Sireau, T., Brach-Papa, C., 2019. Copper, zinc and lead isotope signatures of sediments from a Mediterranean coastal bay impacted by naval activities and urban sources. Appl. Geochem. 111, 104440. https://doi.org/10.1016/j.apgeochem.2019.104440

Araújo, D.F., Ponzevera, E., Weiss, D.J., Knoery, J., Briant, N., Yepez, S., Bruzac, S., Sireau, T., Brach-Papa, C., 2021. Application of Zn isotope compositions in oysters to monitor and quantify anthropogenic Zn bioaccumulation in marine environments over four decades: A “Mussel Watch Program” upgrade. ACS EST Water 4, 1035–1046. https://doi.org/10.1021/acsestwater.1c00010

Araújo, D.F., Knoery, J., Briant, N., Vigier, N., Ponzevera, E., 2022. “Non-traditional” stable isotopes

applied to the study of trace metal contaminants in anthropized marine environments. Mar. Pollut. Bull. 175, 113398. https://doi.org/10.1016/j.marpolbul.2022.113398

Barre, J.P.G., Deletraz, G., Sola-Larrañaga, C., Santamaria, J.M., Bérail, S., Donard, O.F.X., Amouroux, D., 2018. Multi-element isotopic signature (C, N, Pb, Hg) in epiphytic lichens to discriminate atmospheric contamination as a function of land-use characteristics (Pyrénées-Atlantiques, SW France). Environ. Pollut. 243. 961–971. https://doi.org/10.1016/j.envpol.2018.09.003

Bird, 2011. Provenancing anthropogenic Pb within the fluvial environment: Developments and challenges in the use of Pb isotopes. Environ. Int. 37, 802–819. https://doi.org/10.1016/j.envint.2011.02.007

Briffa, J., Sinagra, E., Blundell, R., 2020. Heavy metal pollution in the environment and their toxicological effects on humans. Heliyon 6(9), e04691. https://doi.org/10.1016/j.heliyon.2020.e04691

Bukowiecki, N., Lienemann, P., Hill, M., Figi, R., Richard, A., Furger, M., Ricker, K., Falkenberg, G., Zhao, Y., Cliff, S.S., Prevot, A.S.H., Baltensperger, U., Buchmann, B., Gehrig, R., 2009. Real-world emission factors for antimony and other brake wear related trace elements: Size-segregated values for light and heavy duty vehicles. Environ. Sci. Technol. 43, 8072–8078. https://doi.org/10.1021/es9006096

Desaulty, A.M., Petelet-Giraud, E., 2020. Zinc isotope composition as a tool for tracing sources and fate of metal contaminants in rivers. Sci. Total. Environ. 728, 138599. https://doi.org/10.1016/j.scitotenv.2020.138599

Dong, Y., Rosenbaum, R.K. and Hauschild, M.Z., 2015. Assessment of metal toxicity in marine ecosystems: comparative toxicity potentials for nine cationic metals in coastal seawater. Environ. Sci. Technol. 50, 269–278. https://doi.org/10.1021/acs.est.5b01625

Dong, S., Gonzalez, R.O., Harrison, R.M., Green, D., North, R., Fowler, G., Weiss, D., 2017. Isotopic signatures suggest important contributions from recycled gasoline, road dust and non-exhaust traffic sources for copper, zinc and lead in PM_{10} in London, United Kingdom. Atmos. Environ. 165, 88–98. https://doi.org/10.1016/j.atmosenv.2017.06.020

Dytlow, S., Gorka-Kostrubiec, B., 2021. Concentration of heavy metals in street dust: an implication of using different geochemical background data in estimating the level of heavy metal pollution. Environ. Geochem. Health 43, 521–535. https://doi.org/10.1007/s10653-020-00726-9

Feng, C., Guo, X., Yin, Su, Tian, C., Li, Y., Shen, Z., 2017. Heavy metal partitioning of suspended particulate matter–water and sediment–water in the Yangtze Estuary. Chemosphere 185, 717-725.

https://doi.org/10.1016/j.chemosphere.2017.07.075

Gelhardt, L., Dittmer, U., Welker, A., 2021. Relationship of particle density and organic content in sieve fractions of road-deposited sediments from varying traffic sites based on a novel data set. Sci. Total Environ. 794, 148812. https://doi.org/10.1016/j.scitotenv.2021.148812

Guan, J., Wang, J., Pan, H., Yang, C., Qu, J., Lu, N., Yuan, X., 2018. Heavy metals in Yinma River sediment in a major Phaeozems zone, Northeast China: Distribution, chemical fraction, contamination assessment and source apportionment. Sci. Rep. 8, 12231. https://doi.org/10.1038/s41598-018-30197-z

Huang, Y., Chen, Q., Deng, M., Japenga, J., Li, T., Yang, X., He, Z., 2018. Heavy metal pollution and health risk assessment of agricultural soils in a typical peri-urban area in southeast China. J. Enviro. Manage. 207, 159–168. https://doi.org/10.1016/j.jenvman.2017.10.072

Huber, M., Welker, A., Helmerich, B., 2016. Critical review of heavy metal pollution of traffic area runoff: Occurrence, influencing factors, and partitioning. Sci. Total Environ. 541, 895–919. https://doi.org/10.1016/j.scitotenv.2015.09.033

Hwang, H.M., Fiala, M.J., Park, D., Wade, T.L., 2016. Review of pollutants in urban road dust and stormwater runoff: part 1. Heavy metals released from vehicles. Int. J. Urban Sci. 20(6), 334–360. https://doi.org/10.1080/12265934.2016.1193041

Hwang, D.W., Kim, P.J., Kim, S.G., Sun, C.I., Koh, B.S., Ryu, S.O., Kim, T.H., 2019. Spatial distribution and pollution assessment of metals in intertidal sediments, Korea. Environ. Sci. Pollut. Res. 26, 19379-19388. https://doi.org/10.1007/s11356-019-05177-z

Jeong, H., 2022. Toxic metal concentrations and Cu-Zn-Pb isotopic compositions in tires. J. Anal. Sci. Technol. 13, 2. https://doi.org/10.1186/s40543-021-00312-3

Jeong, H., Choi, J.Y., Lim, J., Shim, W.J., Kim, Y.O., Ra, K., 2020a. Characterization of the contribution of road deposited sediments to the contamination of the close marine environment with trace metals: Case of the port city of Busan (South Korea). Mar. Pollut. Bull. 161(Part A), 111717. https://doi.org/10.1016/j.marpolbul.2020.111717

Jeong, H., Choi, J.Y., Lee, J., Lim, J., Ra, K., 2020b. Heavy metal pollution by road-deposited sediments and its contribution to total suspended solids in rainfall runoff from intensive industrial areas. Environ. Pollut. 265(Part A), 115028. https://doi.org/10.1016/j.envpol.2020.115028

Jeong, H., Choi, J.Y., Lim, J., Ra, K., 2020c. Pollution caused by potentially toxic elements present in road dust from industrial areas in Korea. Atmosphere 11, 1366. https://doi.org/10.3390/atmos11121366

Jeong, H., Choi, J.Y., Lee, J.H., Ra, K., 2020d. Investigation of Pb and Cu isotopes to trace contamination sources from the artificial Shihwa Lake in Korea. J. Coast. Res. SI95, 1122–1127. https://doi.org/10.2112/SI95-218.1

Jeong, H., Choi, J.Y., Ra, K., 2021a. Heavy metal pollution assessment in stream sediments from urban and different types of industrial areas in South Korea. Soil Sed. Contam. 30(7), 804–818. https://doi.org/10.1080/15320383.2021.1893646

Jeong, H., Choi, J.Y., Ra, K., 2021b. Potentially toxic elements pollution in road deposited sediments around the active smelting industry of Korea. Sci. Rep. 11, 7238. https://doi.org/10.1038/s41598-021-86698-x

Jeong, H., Ra, K., 2021a. Multi-isotope signatures (Cu, Zn, Pb) of different particle sizes in road-deposited sediments: a case study from industrial area. J. Anal. Sci. Technol. 12, 39. https://doi.org/10.1186/s40543-021-00292-4

Jeong, H., Ra, K., 2021b. Characteristics of potentially toxic elements, risk assessments, and isotopic compositions (Cu-Zn-Pb) in the PM_{10} fraction of road dust in Busan, South Korea. Atmosphere 12, 1229. https://doi.org/10.3390/atmos12091229

Jeong, H., Ra, K., Choi, J.Y., 2021c. Copper, zinc and lead isotopic delta values and isotope ratios of various geological and biological reference materials. Geostand. Geoanalytical Res. 45(3), 551–563. https://doi.org/10.1111/ggr.12379

Jeong, H., Ra, K., 2022. Source apportionment and health risk assessment for potentially toxic elements in size-fractionated road dust in Busan Metropolitan City, Korea. Environ. Monit. Assess. 194(5), 350. https://doi.org/10.1007/s10661-022-10008-9

Jeong, H., Ryu, J.S., Ra, K., 2022a. Characteristics of potentially toxic elements and multi-isotope signatures (Cu, Zn, Pb) in non-exhaust traffic emission sources. Environ. Pollut. 292(Part A), 118339. https://doi.org/10.1016/j.envpol.2021.118339

Jeong, H., Lee, Y.J., Choi, D.H., Ra, K., 2022b. Spatio- and Temporal distribution of trace metals in seawater and surface sediments around the Geum River estuaary. J. Korean Soc. Mar. Environ. Energy 25, 127-135 (in Korean with English abstract). https://doi.org/10.7846/JKOSMEE.2022.25.2.127.

Ji, X., Abakumov, E., Xie, X., 2019. Atmosphere–ocean exchange of heavy metals and polycyclic aromatic hydrocarbons in the Russian Arctic Ocean. Atmos. Chem. Phys. 19, 13789–13807. https://doi.org/10.5194/acp-19-13789-2019

Jun, E.J., Yi, Y.M., Lee, D.I., Kim, G.Y., 2018. Diagnosis of development projects and water quality

changes in the environmental management sea areas and improvement of impact assessment. J. Korean Soc. Mar. Environ. Saf. 24(6), 726–734 (in Korean with English abstract). https://doi.org/10.7837/kosomes.2018.24.6.726

Kim, M.S., Kim, J.Y., Park, J., Yeon, S.H., Shin, S., Choi, J., 2021. Assessment of pollution sources and contribution in urban dust using metal concentrations and multi-isotope ratios (^{13}C, $^{207/206}Pb$) in a complex industrial port area, Korea. Atmosphere 12, 840. https://doi.org/10.3390/atmos12070840

Kinuthia, G.K., Ngure, V., Beti, D., Lugalia, R., Wangila, A., Kamau, L., 2020. Levels of heavy metals in wastewater and soil samples from open drainage channels in Nairobi, Kenya: community health implication. Sci. Rep. 10, 8434. https://doi.org/10.1038/s41598-020-65359-5

Kwon, E.Y., DeVries T., Galbraith, E.D., Hwang, J., Kum, G., Timmermann, A., 2021. Stable carbon isotopes suggest large terrestrial carbon inputs to the global ocean. Global Biogeochem. Cy. 35, e2020GB00668. https://doi.org/10.1029/2020GB006684

La Colla, N.S., Negrin, V.L., Marcovecchio, J.E., Botte, S.E., 2015. Dissolved and particulate metals dynamics in a human impacted estuary from the SW Atlantic. Estuar. Coast. Shelf Sci. 166(A), 45-55. https://doi.org/10.1016/j.ecss.2015.05.009

Lagerström, M., Ferreira, J., Ytreberg, E., Eriksson-Wiklund, A.K., 2020. Flawed risk assessment of antifouling paints leads to exceedance of guideline values in Baltic Sea marinas. Environ. Sci. Pollut. Res. 27, 27674–27687. https://doi.org/10.1007/s11356-020-08973-0

Lee, Y., Hur, J., Shin, K.H., 2014. Characterization and source identification of organic matter in view of land uses and heavy rainfall in the Lake Shihwa, Korea. Mar. Pollut. Bull. 84, 322–329. https://doi.org/10.1016/j.marpolbul.2014.04.033

Liu, X., Jiang, X., Liu, Q., Teng, A., Xu, W., 2016. Distribution and pollution assessment of heavy metals in surface sediments in the central Bohai Sea, China: a case study. Environ. Earth Sci. 75, 364. https://doi.org/10.1007/s12665-015-5200-2

Maldonado, M.T., Allen, A.E., Chong, J.S., Lin, K., Leus, D., Karpenko, N. and Harris, S.L., 2006. Copper-dependent iron transport in coastal and oceanic diatoms. Limnol. Oceanogr. 51, 1729–1743. https://doi.org/10.4319/lo.2006.51.4.1729

Mao, Y., Ma, Q., Lin, J., Chen, Y., Shu, Q., 2021. Distribution and sources of organic carbon in surface intertidal sediments of the Rudong Coast, Jiangsu Province, China. J. Mar. Sci. Eng. 9, 992. https://doi.org/10.3390/jmse9090992

Marwick, T.T., Tammoh, F., Teodoru, C.R., Borges, A.V., Darchambeau, F., Bouillon, S., 2015. The age

of river-transported carbon: A global perspective. Global Biogeochem. Cy. 29, 122–137. https://doi.org/10.1002/2014GB004911

Moeller, K., Schoenberg, R., Pedersen, R.B., Weiss, D., and Dong, S., 2012. Calibration of the new certified reference materials ERMAE633 and ERM-AE647 for copper and IRMM-3702 for zinc isotope amount ratio determinations. Geostand. Geoanal. Res. 36, 177–199. https://doi.org/10.1111/j.1751-908X.2011.00153.x

Pandiyan, J., Mahboob, S., Govindarajan, M., Al-Ghanim, K.A., Ahmed, Z., Al-Mulhm, N., Jagadheesan, R., Krishnappa, K., 2021. An assessment of level of heavy metals pollution in the water, sediment and aquatic organisms: A perspective of tackling environmental threats for food security. Saudi J. Biol. Sci. 28(2), 1218–1225. https://doi.org/10.1016/j.sjbs.2020.11.072

Park, M.O., Lee, Y.W., Park, J.K., Kim, S.G., Kim, S.S., Lee, S.M., 2018. Changes in water quality in Masan Bay after the introduction of the total pollution load management system. J. Korean Soc. Mar. Environ. Energy 21(2), 139–148 (in Korean with English abstract). https://doi.org/10.7846/JKOSMEE.2018.21.2.139

Pontér, S., Sutliff-Johansson, S., Engström, E., Widerlund, A., Mäki, A., Rodushkina, K., Paulukat, C., Rodushkin, I., 2021. Evaluation of multi-isotope approach as a complement to concentration data within environmental forensics. Minerals 11, 37. https://doi.org/10.3390/min11010037

Posacka, A.M., Semeniuk, D.M., Whitby, H., van den Berg, C.M.G., Gullen, J.T., Orians, K. and Maldonado, M.T., 2017. Dissolved copper (dCu) biogeochemical cycling in the subarctic Northeast Pacific and a call for improving methodologies. Mar. Chem. 196, 47–61. https://doi.org/10.1016/j.marchem.2017.05.007

Pourabadehei, M., Mulligan, C.N., 2016. Selection of an appropriate management strategy for contaminated sediment: a case study at a shallow contaminated harbour in Quebec, Canada. Environ. Pollut. 219, 846–857. https://doi.org/10.1016/j.envpol.2016.08.012

Ra, K., Bang, J.H., Lee, J.M., Kim, K.T., Kim, E.S., 2011. The extent and historical trend of metal pollution recorded in core sediments from the artificial Lake Shihwa, Korea. Mar. Pollut. Bull. 62(8), 1814–1821. https://doi.org/10.1016/j.marpolbul.2011.05.010

Ra, K., Kim, J.K., Hong, S.H., Yim, U.H., Shim, W.J., Lee, S.Y., Kim, Y.O., Lim, J., Kim, E.S., Kim, K.T., 2014. Assessment of pollution and ecological risk of heavy metals in the surface sediments of Ulsan Bay, Korea. Ocean Sci. J. 49, 279–289. https://doi.org/10.1007/s12601-014-0028-3

Rahman, Z., Singh, V.P., 2019. The relative impact of toxic heavy metals (THMs) (arsenic (As),

cadmium (Cd), chromium (Cr)(VI), mercury (Hg), and lead (Pb)) on the total environment: an overview. Environ. Monit. Assess. 191, 419. https://doi.org/10.1007/s10661-019-7528-7

Rudnick, R.L., Gao, S., 2003. Composition of the continental crust. In: Heinrich, D.H., Karl, K.T. (Eds.), Treatise on Geochemistry, Pergamon, Oxford, pp. 1–64.

Schiff, K., Diehl, D., Valkirs, A., 2004. Copper emissions from antifouling paint on recreational vessels. Mar. Pollut. Bull. 48, 371–377. https://doi.org/10.1016/j.marpolbul.2003.08.016

Schleicher, N.J., Dong, S., Packman, H., Little, S.H., Gonzalez, R.O., Najorka, J., Sun, Y., Weiss, D.J., 2020. A global assessment of copper, zinc, and lead isotopes in mineral dust sources and aerosols. Front. Earth Sci. 8, 167. https://doi.org/10.3389/feart.2020.00167

Souto-Oliveira, C.E., Babinski, M., Araújo, D.F., Andrade, M.F., 2018. Multi-isotopic fingerprints (Pb, Zn, Cu) applied for urban aerosol source apportionment and discrimination. Sci. Total Environ. 626, 1350–1366. https://doi.org/10.1016/j.scitotenv.2018.01.192

Souto-Oliveira, C.E., Babinski, M., Araújo, D.F., Weiss, D.J., Ruiz, I.R., 2019. Multi-isotope approach of Pb, Cu and Zn in urban aerosols and anthropogenic sources improves tracing of the atmospheric pollutant sources in megacities. Atmos. Environ. 198, 427–437. https://doi.org/10.1016/j.atmosenv.2018.11.007

Sutherland, R.A., 2000. Bed sediment-associated trace metals in an urban stream, Oahu, Hawaii. Environ. Geol. 39, 611–627. https://doi.org/10.1007/s002540050473

Suvetha, M., Charles, P.E., Vinothkannan, A., Rajaram, R., Paray, B.A., Ali, S., 2022. Are we at risk because of road dust? An ecological and health risk assessment of heavy metals in a rapid growing city in South India. Environ. Adv. 7, 100165. https://doi.org/10.1016/j.envadv.2022.100165

Tang, H., Ke, Z., Yang, M., Wang, W., Nie, H., Li, B., Zhang, J., Xu, X., Wang, J., 2018. Concentrations, distribution, and ecological risk assessment of heavy metals in Daya Bay, China. Water 10(6), 780. https://doi.org/10.3390/w10060780

Tomlinson, D.L., Wilson, J.G., Harris, C.R., Jeffrey, D.W., 1980. Problems in the assessment of heavy-metal levels in estuaries and the formation of a pollution index. Helgol. Meeresunters. 33, 566–575. https://doi.org/10.1007/BF02414780

Vanderstraeten, A., Bonneville, S., Gili, S., de Jong, J., Debouge, W., Claeys, P., Mattielli, N., 2020. First multi-isotopic (Pb-Nd-Sr-Zn-Cu-Fe) characteristics of dust reference materials (ATD and BCR-723): a multi-column chromatographic method optimised to trace mineral and anthropogenic dust sources. Geostand. Geoanal. Res. 44 (2), 307–329. https://doi.org/10.1111/ggr.12320

Wang, L., Jin, Y., Weiss, D.J., Schleicher, N.J., Wilcke, W., Wu, L., Guo, Q., Chen, J., O'Connor, D., Hou, D., 2021a. Possible application of stable isotope compositions for the identification of metal sources in soil. J. Hazard. Mat. 407, 124812. https://doi.org/10.1016/j.jhazmat.2020.124812

Wang, J., Qin, M., Huang, T., Tu, N., Li, B., 2021b. Particle size distribution and pollutant dissolution characteristics of road-deposited sediment in different land-use districts: a case study of Beijing. Environ. Sci. Pollut. Res. 28, 38497–38505. https://doi.org/10.1007/s11356-021-13426-3

Wang, Q., Zhang, Q., Dzakpasu, M., Chang, N., Wang, X., 2019. Transferral of HMs pollution from road-deposited sediments to stormwater runoff during transport processes. Front. Environ. Sci. Eng. 13(1), 13. https://doi.org/10.1007/s11783-019-1091-x

Wang, Z., Chen, J., Zhang, T., 2017. Cu isotopic composition in surface environments and in biological systems: a critical review. Int. J. Environ. Res. Public Health 14, 538. https://doi.org/10.3390/ijerph14050538

Wicke, D., Cochrane, T.A., O'Sulivanm A.D., 2012. Atmospheric deposition and storm induced runoff of heavy metals from different impermeable urban surfaces. J. Environ. Monit. 14, 209-216. https://doi.org/10.1039/C1EM10643K

Wiederhold, J.G., 2015. Metal Stable Isotope Signatures as Tracers in Environmental Geochemistry. Environ. Sci. Technol. 49(5), 2606-2624. https://doi.org/10.1021/es504683e

Wu, Z., Zhang, L., Xia, T., Jia, X., Wang, S., 2020. Heavy metal pollution and human health risk assessment at mercury smelting sites in Wanshan district of Guizhou Province, China. RSC Adv. 10, 23066. https://doi.org/10.1039/D0RA01004A

Yang, Q., Li, Z., Lu, X., Duan, Q., Huang, L, Bi, J., 2018. A review of soil heavy metal pollution from industrial and agricultural regions in China: Pollution and risk assessment. Sci. Total Environ. 642, 690–700. https://doi.org/10.1016/j.scitotenv.2018.06.068

Yin, N.H., Sivry, Y., Benedetti, M.F., Lens, P.N.L., van Hullebusch, E.D., 2016. Application of Zn isotopes in environmental impact assessment of Zn–Pb metallurgical industries: a mini review. Appl. Geochem. 64, 128–135. https://doi.org/10.1016/j.apgeochem.2015.09.016

Zhao, H., Ma, Y., Fang, J., Hu, L., Li, X., 2022. Particle size distribution and total suspended solid concentrations in urban surface runoff. Sci. Total Environ. 815, 152533. https://doi.org/10.1016/j.scitotenv.2021.152533

Zimnoch, M., Samek, L., Furman, L., Styszko, K., Skiba, A., Gorczyca, Z., Galkowski, M., Rozanski, K., Konduracka, E., 2020. Application of natural carbon isotopes for emission source apportionment of

carbonaceous particulate matter in urban atmosphere: a case study from Krakow, Southern Poland. Sustainability 12, 5777. https://doi.org/10.3390/su12145777

Zoller, W.H., Gladney, E.S., Duce, R.A., 1974. Atmospheric concentrations and sources of trace metals at the South Pole. Science 183, 199–201. https://www.science.org/doi/10.1126/science.183.4121.198

[List of Figures]

[List of Tables]

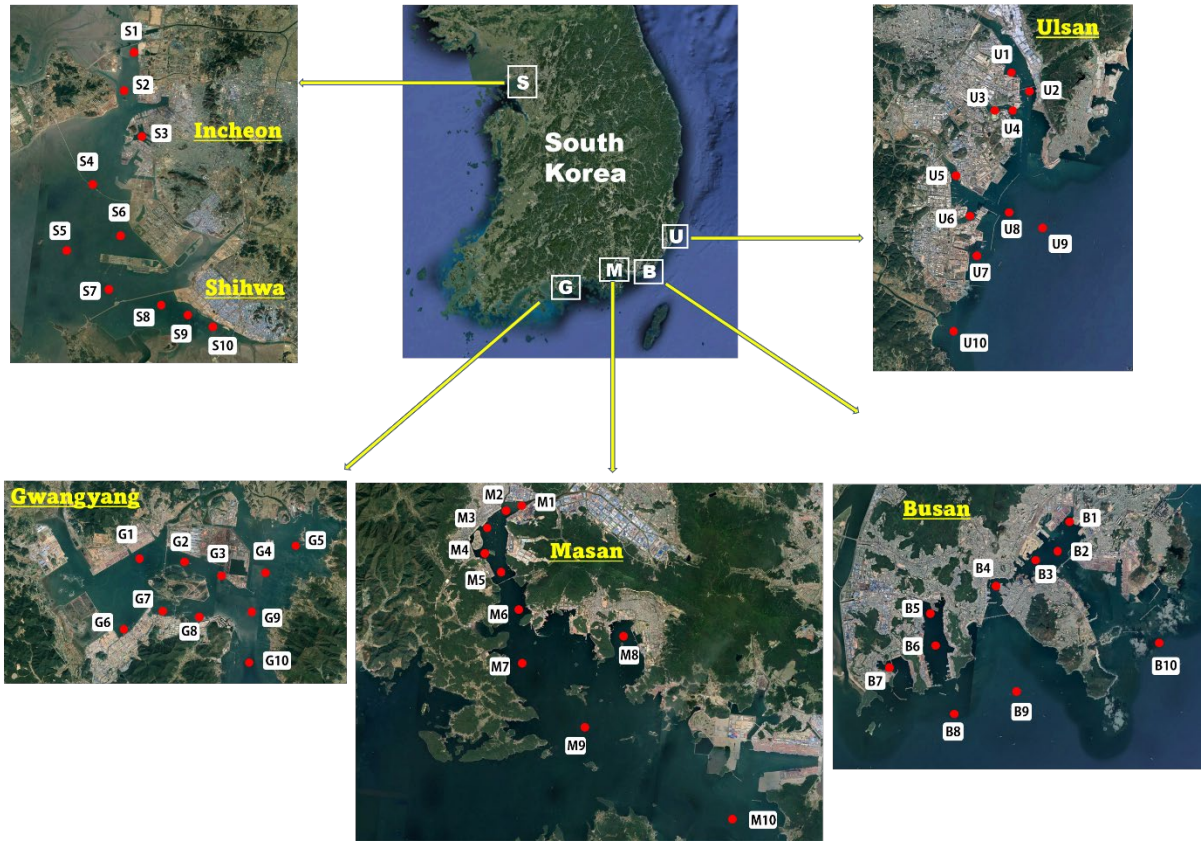

Fig. 1. Sampling locations of surface sediments from 5 special managements areas (SMAs) in Korea (base map from Google Earth).

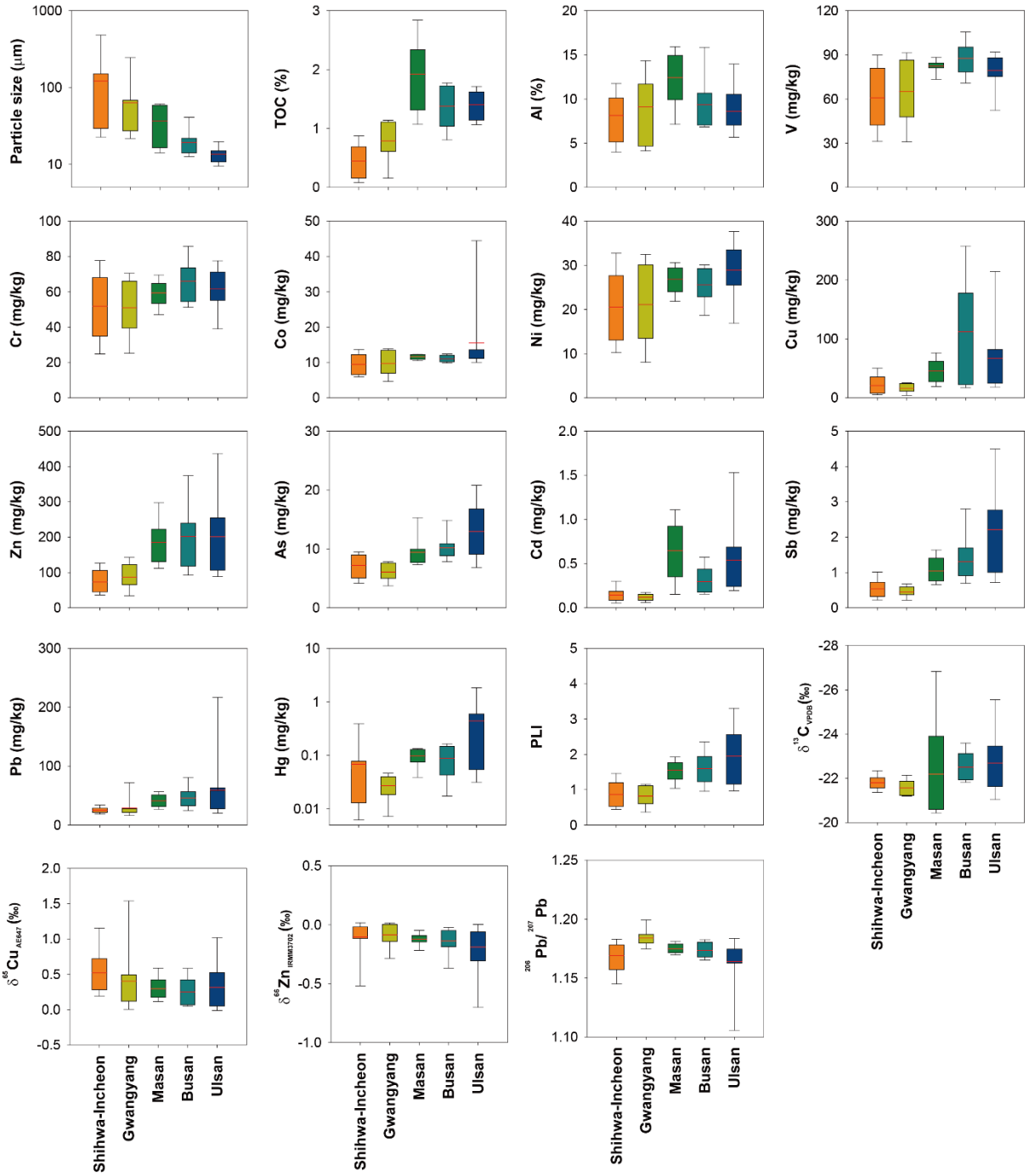

Fig. 2. Comparison of particle size, total organic carbon (TOC), heavy metals, pollution load index (PLI), and isotopic composition for C, Cu, Zn, and Pb in sediments of this study. Red line indicates the mean value.

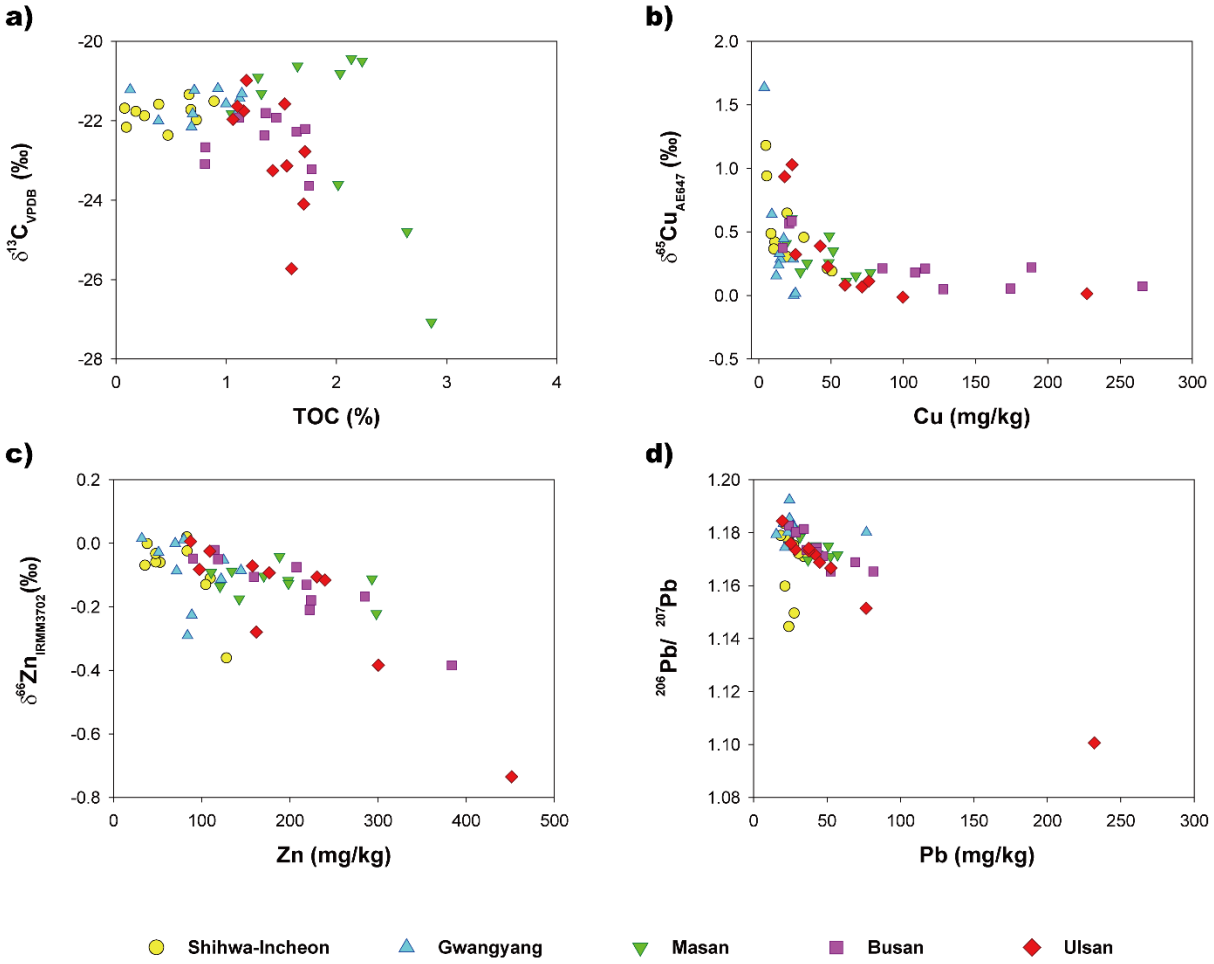

Fig. 3. Bi-plots between concentrations and isotopic compositions for C (a), Cu (b), Zn (c), and Pb (Pb) in surface sediments of this study.

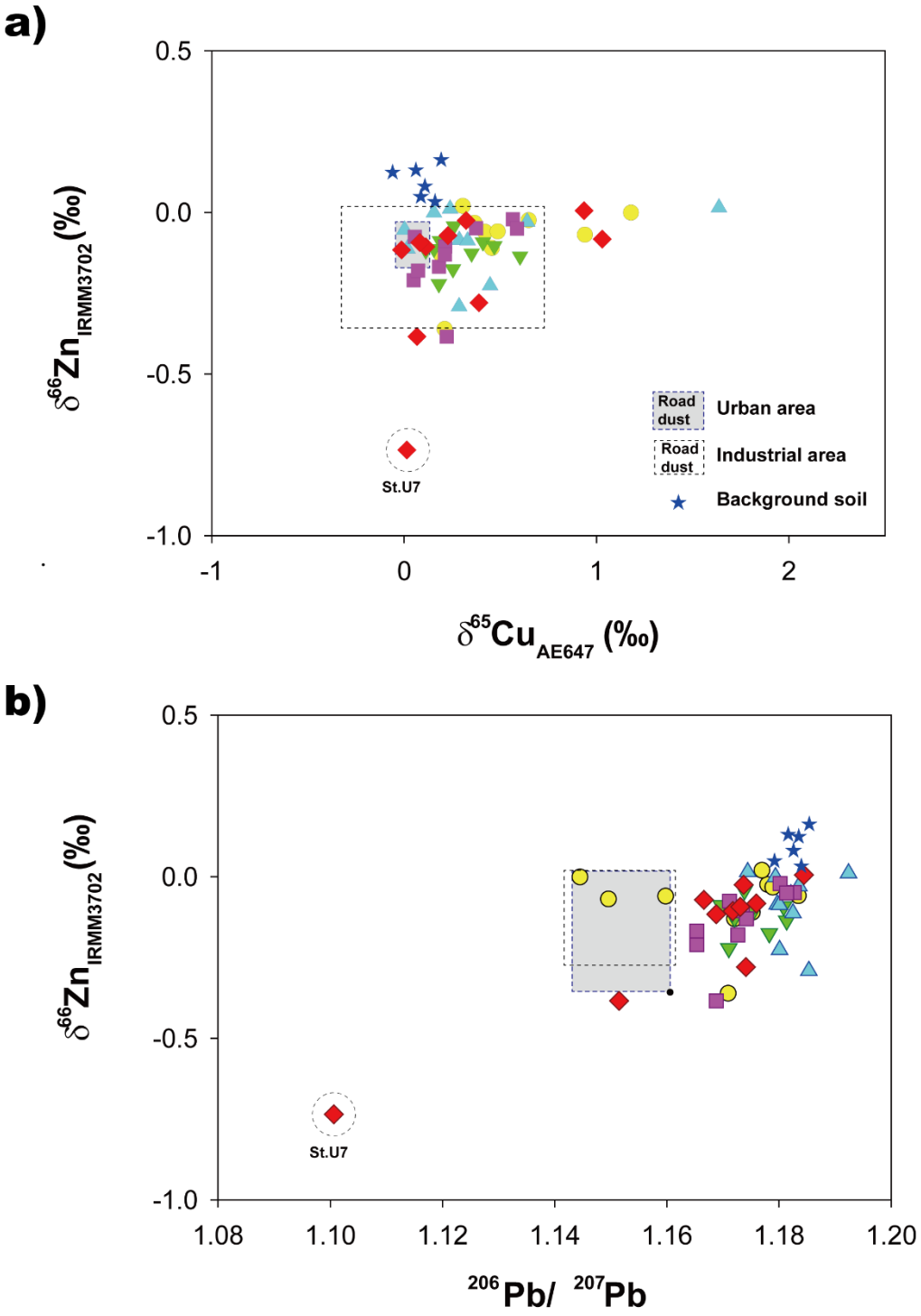

Fig. 4. Biplots of $\delta^{65}Cu$ versus $\delta^{66}Zn$ (a) and $^{206}Pb/^{207}Pb$ versus $\delta^{66}Zn$ of this study and other literature data (background soil and road dust from urban (Jeong and Ra, 2021b), and road dust from industrial area of Korea (Jeong and Ra, 2021b)). Symbols are the same as Fig. 3.

Table 1. Comparison of mean concentrations (minimum and maximum value in parenthesis) and coefficient of variation (CV; %) values for TOC and heavy metals in surface sediments of the study area.

	Particle size (μm)	**TOC (%)**	**V (mg/kg)**	**Cr (mg/kg)**	**Co (mg/kg)**	**Ni (mg/kg)**	**Cu (mg/kg)**	**Zn (mg/kg)**	**As (mg/kg)**	**Cd (mg/kg)**	**Sb (mg/kg)**	**Pb (mg/kg)**	**Hg (mg/kg)**
Shihwa-Incheon	51 (22–493) 173%	0.44 (0.08–0.89) 65%	60.9 (31.2–90.1) 36%	51.9 (24.7–78.0) 38%	9.4 (5.8–13.7) 32%	20.6 (10.0–32.9) 41%	20.9 (4.9–50.9) 80%	73.2 (35.7–128) 45%	7.2 (4.1–9.5) 27%	0.14 (0.05–0.31) 52%	0.5 (0.2–1.0) 49%	25.3 (18.5–34.4) 19%	0.07 (0.01–0.43) 185%
Gwangyang	63 (21–262) 116%	0.79 (0.13–1.14) 43%	64.9 (29.7–91.5) 32%	51.1 (24.5–70.7) 30%	9.8 (4.5–13.9) 33%	21.1 (7.5–32.6) 40%	15.9 (3.8–25.4) 44%	86.8 (32.0–144) 40%	6.1 (3.6–7.8) 24%	0.12 (0.06–0.18) 32%	0.4 (0.2–0.7) 31%	28.9 (15.5–76.9) 60%	0.03 (0.01–0.05) 47%
Masan	37 (14–61) 54%	1.92 (1.05–2.86) 31%	82.5 (72.9–88.6) 5%	59.4 (46.7–70.0) 12%	11.7 (10.4–12.3) 6%	26.8 (21.8–30.6) 12%	45.8 (18.9–77.3) 42%	185 (111–298) 36%	9.4 (7.3–15.9) 26%	0.65 (0.15–1.12) 52%	1.0 (0.7–1.6) 33%	41.2 (26.7–57.2) 25%	0.10 (0.04–0.13) 35%
Busan	19 (12–43) 47%	1.38 (0.81–1.78) 27%	87.6 (70.5–106) 13%	66.1 (51.0–86.8) 17%	11.2 (9.9–12.5) 8%	25.6 (18.4–30.2) 15%	113 (16.7–265) 72%	202 (89.9–384) 44%	10.2 (7.7–15.2) 20%	0.29 (0.15–0.58) 54%	1.3 (0.7–2.9) 51%	46.0 (24.1–81.5) 39%	0.09 (0.01–0.16) 59%
Ulsan	14 (9–20) 23%	1.40 (1.06–1.71) 18%	79.4 (50.2–92.3) 15%	61.6 (37.6–78.2) 19%	15.5 (9.9–47.9) 73%	28.9 (16.3–38.1) 22%	69.1 (17.9–227) 89%	201 (87.4–451) 55%	13.0 (6.8–20.9) 38%	0.54 (0.19–1.63) 78%	2.2 (0.7–4.6) 54%	59.7 (19.6–232) 105%	0.44 (0.03–1.85) 161%
Total	51 (9–493) 173%	1.19 (0.08–2.86) 54%	75.1 (29.7–106) 24%	58.5 (24.5–86.8) 25%	11.5 (4.5–47.9) 50%	24.6 (7.5–38.1) 28%	52.8 (3.8–265) 109%	150 (32.0–451) 61%	9.2 (3.6–20.9) 40%	0.35 (0.05–1.63) 93%	1.1 (0.2–4.5) 80%	40.2 (15.5–232) 79%	0.14 (0.01–1.35) 239%

Table 2. Mean values of enrichment factor (EF) for heavy metals in the sediments of this study.

	V	Cr	Co	Ni	Cu	Zn	As	Cd	Sb	Pb	Hg
Shihwa-Incheon	0.6	0.6	0.6	0.4	0.7	1.1	1.7	1.6	1.3	1.7	1.3
Gwangyang	0.6	0.5	0.5	0.4	0.5	1.2	1.3	1.2	1.1	1.7	0.5
Masan	0.6	0.5	0.5	0.4	1.1	1.8	1.4	4.4	1.8	1.6	1.3
Busan	0.8	0.7	0.6	0.5	3.5	2.7	1.9	3.1	3.1	2.5	1.7
Ulsan	0.8	0.7	1.0	0.6	2.7	3.2	2.6	6.6	5.5	4.1	10.7

EF<1; deficiency

1<EF<2; minimal enrichment

2<EF<5; moderate enrichment

5<EF<10; significant enrichment

5<EF<20; significant enrichment

Table 3. Comparison of mean concentrations (minimum and maximum value in parenthesis) for C, Cu, Zn and Pb isotopic compositions in surface sediments of the study area.

Regions	**$\delta^{13}C_{VPDB}$ (‰)**	**$\delta^{65}Cu_{AE647}$ (‰)**	**$\delta^{66}Zn_{IRMM3702}$ (‰)**	**$^{206}Pb/^{207}Pb$**
Shihwa-Incheon	–21.80 (–22.37 to –21.34)	0.52 (0.19 to 1.18)	–0.08 (–0.36 to 0.02)	1.1690 (1.1445 to 1.1835)
Gwangyang	–21.57 (–22.15 to –21.19)	0.40 (0.00 to 1.64)	–0.09 (–0.29 to 0.02)	1.1820 (1.1744 to 1.1924)
Masan	–22.19 (–27.07 to –20.43)	0.30 (0.11 to 0.60)	–0.12 (–0.22 to –0.04)	1.1749 (1.1697 to 1.1814)
Busan	–22.51 (–23.64 to –21.81)	0.25 (0.05 to 0.59)	–0.14 (–0.38 to –0.02)	1.1736 (1.1654 to 1.1827)
Ulsan	–22.69 (–25.72 to –20.98)	0.32 (–0.01 to 1.03)	–0.19 (–0.73 to 0.01)	1.1641 (1.1006 to 1.1844)
Total	–22.15 (–27.07 to –20.43)	0.36 (–0.01 to 1.64)	–0.12 (–0.73 to 0.02)	1.1727 (1.1006 to 1.1924)

Table 4. Pearson's correlation matrix between particle size, TOC, metals and isotopic compositions (C, Cu, Zn, and Pb) in all sediments (N=50) of this study. Superscript (*) indicates that correlation is significant at the 0.01 level (2-tailed).

	Size	TOC	V	Cr	Co	Ni	Cu	Zn	As	Cd	Sb	Pb	Hg	$\delta^{13}C$	$\delta^{65}Cu$	$\delta^{66}Zn$	$^{206}Pb/^{207}Pb$
Size	-																
TOC	-0.47*	-															
V	-0.66*	0.69*	-														
Cr	-0.64*	0.47*	0.88*	-													
Co	-0.32	0.30	0.46*	0.50*	-												
Ni	-0.60*	0.55*	0.88*	0.90*	0.59*	-											
Cu	-0.28	0.43*	0.41*	0.37*	0.20	0.26	-										
Zn	-0.38*	0.68*	0.51*	0.45*	0.43*	0.42*	0.80*	-									
As	-0.25	0.60*	0.54*	0.34	0.38*	0.51*	0.41*	0.55*	-								
Cd	-0.20	0.66*	0.25	0.15	0.29	0.23	0.49*	0.82*	0.42*	-							
Sb	-0.33*	0.53*	0.44*	0.33	0.40*	0.40*	0.55*	0.73*	0.74*	0.60*	-						
Pb	-0.16	0.27	0.08	0.00	0.27	0.01	0.64*	0.75*	0.30	0.72*	0.60*	-					
Hg	-0.15	0.13	0.06	0.10	0.74*	0.18	0.38*	0.58*	0.26	0.56*	0.51*	0.73*	-				
$\delta^{13}C$	0.15	-0.42*	-0.15	0.03	-0.13	-0.02	-0.22	-0.34	-0.68*	-0.23	-0.44*	-0.18	-0.11	-			
$\delta^{65}Cu$	0.65*	-0.50*	-0.61*	-0.57*	-0.36	-0.55*	-0.48*	-0.56*	-0.38*	-0.39*	-0.47*	-0.33	-0.25	0.16	-		
$\delta^{66}Zn$	0.23	-0.26	-0.20	-0.18	-0.40*	-0.18	-0.59*	-0.71*	-0.35	-0.59*	-0.51*	-0.81*	-0.68*	0.18	0.39*	-	
$^{206}Pb/^{207}Pb$	-0.30	-0.01	0.21	0.22	-0.21	0.17	-0.47*	-0.52*	-0.22	-0.56*	-0.47*	-0.78*	-0.69*	0.10	0.06	0.62*	-